First Observation of Forces on Three-Level Atoms in Raman Resonant Standing-Wave Optical Fields

P. R. Hemmer,[1] M. S. Shahriar,[2] M. G. Prentiss,[3] D. P. Katz,[4] K. Berggren,[3] J. Mervis,[3] and N. P. Bigelow[5]

[1]*Rome Laboratory, Hanscom Air Force Base, Bedford, Massachusetts 01731*
[2]*Research Laboratory of Electronics, Massachusetts Institute of Technology, Cambridge, Massachusetts 02139*
[3]*Department of Physics, Harvard University Cambridge, Massachusetts 02138*
[4]*Division of Applied Sciences, Harvard University, Cambridge, Massachusetts 02138*
[5]*Department of Physics and Astronomy, University of Rochester, Rochester, New York 14627*
(Received 26 December 1991)

A sodium atomic beam is deflected by two optical standing-wave fields which excite near resonance Raman transitions. Observed deflections are consistent with theoretical predictions of a long-range dc component of the force on a three-level atom in the Λ configuration. The low laser intensities (and small detunings) used, combined with observed evidence of damping in the three-level Λ system, may ultimately lead to the design of high-density, all optical traps wherein the atoms would be mostly in the dark state.

PACS numbers: 32.80.Pj, 42.50.Vk

The interaction of two laser fields with a three-level atom in the Λ configuration has been of increasing interest in recent years. Forces due to counterpropagating traveling waves (TW) have been used to cool atoms below the single photon recoil limit [1], and to demonstrate a matter wave interferometer [2]. Recently, theoretical solutions of the steady-state optical Bloch equations have shown that the semiclassical force on a stationary three-level atom in standing-wave (SW) fields is unbounded, with spatial variations on length scales both much longer and much shorter than an optical wavelength [3,4].

In this paper we show experimental verification of the existence of the long-range component of this force by deflecting an atomic beam of three-level sodium atoms using two Raman resonant SW laser fields. This long-range force is the force averaged over an optical wavelength. In addition, we show the existence of damping forces. These observations are important for several reasons. First, the deflecting force is stimulated so that it can be made arbitrarily large. With the coexistence of semiclassical damping forces, this opens the possibility of developing deeper neutral atom traps. Moreover, the Raman interaction tends to drive atoms into the transparent (or "dark") state [5,6], so that atoms in a Raman trap would be mostly in the ground states. As a result [7,8], the Raman force may ultimately lead to high densities of cold and dark atoms in traps. Such a dense collection of atoms in transparent superposition states could find applications as novel, low-intensity nonlinear optical materials [9,10], as well as in a Raman-atomic clock [11].

Previously, the stimulated force due to bichromatic SW laser fields was found to induce observable deflection of an atomic beam of two-level sodium atoms [12]. It has also been proposed that three-level atoms in the V configuration could be deflected using two counterpropagating TW fields [13]. Both of these schemes require strong laser fields and large laser detunings, and no significant damping forces are predicted or observed. In contrast, the scheme presented here uses nearly resonant SW fields, so relatively large forces (deflecting or trapping) can be obtained with low laser intensities (on the order of the saturation intensity). In fact, the laser intensities and detunings used in this demonstration experiment are not very different from those used in existing neutral atom traps.

A schematic diagram of the three-level Λ system is shown in Fig. 1(a). In this experiment, the states $|a\rangle$, $|b\rangle$, and $|e\rangle$ are, respectively, the $3^2S_{1/2}(F=1)$, $3^2S_{1/2}(F=2)$, and $3^2P_{1/2}(F=2)$ states of sodium. Laser detunings are expressed in terms of common mode (or correlated) detuning δ and difference frequency detuning Δ, defined, respectively, as $\delta=(\delta_1+\delta_2)/2$ and $\Delta=\delta_1-\delta_2$, where δ_i is the detuning of the field at ω_i. An important parameter is the phase difference between the two standing waves: $\chi=(k_2-k_1)z$, where $k_i=\omega_i/c$ and z is the position of the atom. It can be shown that for conditions

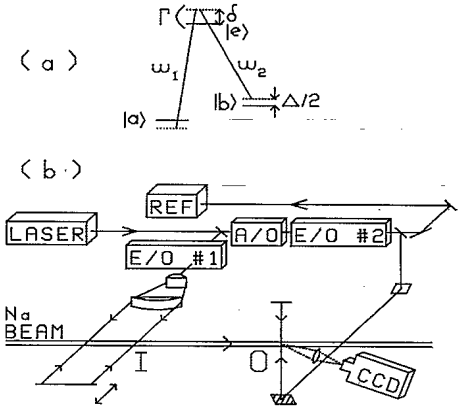

FIG. 1. (a) Schematic of the three-level Λ system. (b) Perspective diagram of the experimental setup. I is the interaction zone, O is the observation zone, REF is a reference atomic beam and associated optics, and CCD is a charge coupled device video camera.

corresponding to our experiment (e.g., Rabi frequencies and Δ comparable to Γ) the long-range component of this force varies basically as $\Delta\sin(2\chi)$.

The experimental setup is shown schematically in Fig. 1(b). A sodium oven at 400°C is used to generate the atomic beam which is collimated to about 3 mrad (FWHM) by two 1.5-mm-diam pinholes separated by 55 cm. Windows are provided in the atomic beam apparatus for an interaction zone [labeled I in Fig. 1(b)] and an observation zone (labeled O) 18 and 58 cm, respectively, from the second pinhole. An argon pumped ring dye laser is used to generate the optical field at ω_1 (590 nm). The field at ω_2 is generated with an electro-optic phase modulator (E/O_1) driven near the 1772-MHz sodium ground-state hyperfine frequency. The drive voltage to E/O_1 is adjusted so that the fundamental and the two sidebands have equal laser power, each about 30% of the input power. To change ω_1 the laser is offset locked by sending a portion of the laser output through an acousto-optic modulator (A/O) followed by a second E/O (E/O_2), as shown, to generate two equal sidebands, one of which is near ω_1. This sideband is locked to an atomic beam reference (labeled REF) so that by changing the frequency of the A/O both ω_1 and ω_2 can be tuned together.

To provide a long interaction time, the laser emerging from E/O_1 is expanded to a line of approximately uniform intensity (20% maximum variation) with a length of 4.1 cm and a width of about 0.24 mm (FWHM) at the atomic beam. This expanded beam then intersects the atomic beam at a right angle, and is retroreflected by a translatable mirror on the opposite side of the atomic beam. This produces SW fields with a variable phase difference between the ω_1 and ω_2 components at the atomic beam. Maximum laser power in the incoming interaction beam is about 70 mW. This corresponds to a laser intensity of about 200 mW/cm^2 for each component at ω_1 and ω_2 in both the incoming and retroreflected laser fields. Laser polarization is circular (both ω_1 and ω_2), but with a magnetic field of about 1 G oriented perpendicular to the propagation directions of both the laser beam and the atomic beam. In this configuration [14], all σ and π transitions are excited so as to prevent population trapping in the $F=2, m_F=2$ ground-state sublevel.

To detect the effects of the interaction on the atomic beam, a portion of the reference laser beam (emerging from E/O_2) is split off to form a standing-wave probe field which intersects the atomic beam in the observation region. To minimize Doppler shifts the probe beam is made perpendicular to both the interaction laser beam and the atomic beam. Fluorescence generated by this probe field is imaged onto a CCD video camera, as shown in Fig. 1(b). The imaging system is slightly off axis with the atomic beam propagation direction to avoid detecting stray light from the interaction zone. To ensure that the fluorescence intensity is an accurate measure of the atomic density, both ground-state sublevel populations are probed via the uncoupled transitions: $3^2S_{1/2}(F=1) \rightarrow 3^2P_{1/2}(F=2)$ and $3^2S_{1/2}(F=2) \rightarrow 3^2P_{1/2}(F=1)$, which are separated by 1960 MHz. These are excited by applying a 980-MHz signal to E/O_2 to generate sidebands separated by the required 1960 MHz. Typical probe laser power is about 0.1 mW in a cylindrical beam of about 1 mm×20 mm in size.

Atomic beam deflection data are shown in Fig. 2. Each data trace is a digitized line from a single stored video frame. For these data we chose to use the maximum laser power available (200 mW/cm^2) in the interaction zone. The detunings were then optimized ($\Delta=-16$ MHz, $\delta=4$ MHz) to observe the cleanest deflection.

In Fig. 2 the top trace shows the atomic beam profile with the interaction laser beam blocked. The measured beam width of 3 mm is consistent with the geometric estimate. The next four traces show the deflection obtained for SW fields having relative phase shifts of $\chi=0$, $\pi/4$, $\pi/2$, and $3\pi/4$ as labeled. The $\chi=0$ trace, which corresponds to in-phase SW fields, is obtained with the retroreflection mirror 17 cm (or one complete optical beat wavelength) from the atomic beam. The bottom trace in the figure is obtained with the retroreflected interaction laser beam blocked. This data trace shows the spontaneous deflection induced by copropagating TW fields at ω_1 and ω_2, and is included for comparison. The peak atomic beam deflection in this case is about 3 mrad.

Examination of the data in Fig. 2 reveals several important points. First, the atomic beam profile for $\chi=\pi/4$

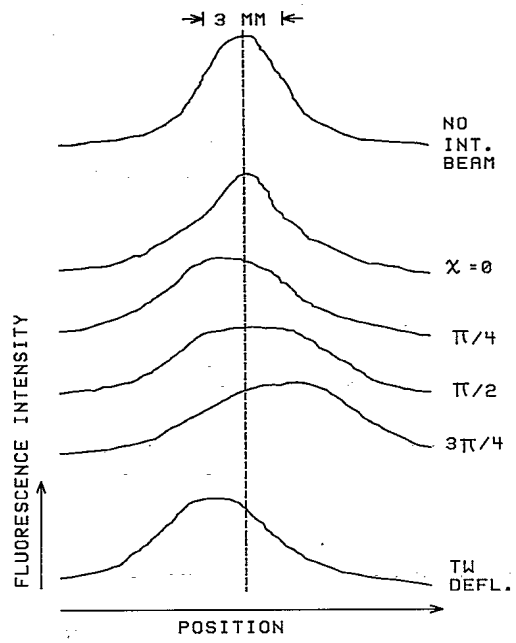

FIG. 2. Atomic beam deflection data obtained using setup of Fig. 1(b). Traces are obtained by digitizing single lines of stored video images. Standing-wave phase shifts χ are as labeled. Laser intensity is 200 mW/cm^2 at each frequency, with detunings $\Delta=-16$ MHz and $\delta=4$ MHz.

shows clear asymmetry and centroid deflection to the left, which is the direction of the incoming interaction laser beam. In contrast, for $\chi=3\pi/4$, the asymmetry and centroid shift are similar in magnitude, but in the opposite direction. For $\chi=0$ and $\pi/2$, the centroids are not shifted. Reversal of asymmetry and centroid shift are also observed (not shown) for fixed values of χ (e.g., $\chi=\pi/4$ or $3\pi/4$) when the laser difference detuning Δ is reversed in sign. For TW Raman fields the deflection is not reversed with Δ. These observations are in agreement with theoretical predictions.

Quantitative comparison of the magnitudes of the observed deflections in Fig. 2 with theory is difficult for two reasons: First, sodium is not a pure three-level system but rather has 13 m levels with 21 allowed optical transitions for the laser polarization and magnetic-field orientation used in this experiment. Since each optical transition has a different matrix element, different Rabi frequencies apply. Second, the observed peak deflection angle (when $\chi=\pi/4$ or $3\pi/4$) is about 4 mrad, which corresponds to a final transverse velocity of about 280 cm/s or a Doppler shift of about 5 MHz$=\Gamma/2$. Since this is comparable to Γ, typical values of Δ, and the Rabi frequencies, the stationary atom assumption used to derive the theoretical force is not strictly valid. Nonetheless, to get an idea about the size of the deflection, we have used the $v=0$ approximation to find the force for a representative transition $[3^2S_{1/2}(F=1,m_F=0)\rightarrow 3^2P_{1/2}(F=2,m_F=1)\rightarrow 3^2S_{1/2}(F=2,m_F=0)]$. Under the experimental conditions of Fig. 2, the Rabi frequencies at the antinodes of each SW is about 21 MHz$=2.1\Gamma$ for each leg of this transition. Assuming the force remains constant over the deflection zone, we find a maximum deflection (at $\chi=\pi/4$ or $3\pi/4$) of 5.6 mrad, which is consistent with the observed maximum deflection of about 4 mrad in Fig. 2.

We have also observed deflection of magnitude similar to those in Fig. 2 at lower laser intensities with different values of laser detunings. For example, deflections as large as 4 mrad (not shown) were observed for $\chi=\pi/4$ with a laser intensity of 53 mW/cm^2, and detunings of $\Delta=-5$ MHz and $\delta=0$. Theory for these conditions predicts a deflection of about 5.2 mrad, which again is consistent with the observation. However, we have not observed any SW deflection larger than about 4 mrad in the present setup, even though stationary atom theory predicts larger deflections for some of the experimental conditions we have tried (e.g., $\Delta=\Gamma$, $\delta=0$, and the same laser intensity as in Fig. 2). At present, we have not identified the reason for this.

Experimentally, it is often difficult to observe clean deflection as in the data of Fig. 2, because of the presence of accelerating and damping forces. One example of strong damping is shown in Fig. 3 where $\Delta=-3$ MHz, $\delta=11$ MHz, and the laser intensity is 200 mW/cm^2 (as in Fig. 2). As can be seen, when the phase is $\chi=3\pi/4$, the damping is the strongest [15]. In fact, these data correspond to an atomic beam width of 2 mm in the observation zone, which is also approximately the width expected at the interaction zone, based on geometric considerations. This implies that the atomic beam divergence has been greatly reduced at the interaction zone. However, our ability to determine the residual divergence of the atomic beam from the data in Fig. 3 is limited to an accuracy of about 0.5 mrad because of roughly 10% uncertainty in measuring the linewidths. This gives an upper limit of the velocity spread of about ± 20 cm/s, which is barely below the Doppler cooling limit (30 cm/s). Clearly, more accurate measurements are necessary. Finally, note that there is virtually no deflection observed in Fig. 3, even though our stationary atom theory predicts a large deflection for $\chi=3\pi/4$ under these conditions. We believe this is due to masking of the deflection force by the strong damping force.

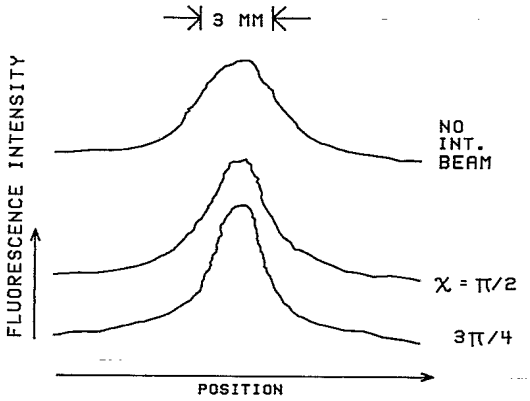

FIG. 3. Data showing evidence of strong damping forces. Laser-laser intensity is 200 mW/cm^2, and detunings are $\Delta=-3$ MHz and $\delta=11$ MHz.

As we have pointed out, the deflection force changes sign when the sign of Δ is reversed. This property can be of help in designing an all optical trap. Briefly, one can conceivably design a magnetic-field gradient such that the value of Δ is antisymmetric with respect to the zero-field point, which would be the trap center. The dimension of the trap should be small enough (compared to 17 cm) so that the value of χ remains a constant (e.g., $3\pi/4$). The deflection force would thus always push the atoms towards the trap center, acting as a restoring force. Near the trap center, Δ is small, which corresponds to the largest observed damping forces for the optimal value of δ. Since $\Delta=0$ in the trap center, slowly moving atoms at this point would be mostly in the dark state. Note that, as in the case of existing two-level standing-wave traps [16], this scheme could potentially work even if deflection and damping are not present at the same position. Thus, the fact that deflection and damping are not observed simultaneously in Fig. 3 is not a serious concern at present. Generalizing this scheme to three dimensions is of course a nontrivial problem, and will be the subject of further investigation.

In summary, we have observed phase-dependent

deflection of a sodium atomic beam by two standing waves, simultaneously near resonance with both components of a Λ three-level system. Qualitative agreement between theory and experiment is achieved, even though sodium is not a pure three-level system and the stationary atom assumption is violated. In addition, we have observed phase-dependent cooling, being maximum at the phase where the deflection is maximum. Potential applications to high-density, dark atom traps are currently being investigated, both theoretically and experimentally.

We wish to acknowledge the invaluable contributions of Professor S. Ezekiel of MIT and John Kierstead. This work was supported by Rome Laboratory Contract No. F19628-89-K-0300 and Office of Naval Research Grant No. ONR-N0014-91-J-1808.

[1] A. Aspect, E. Arimondo, R. Kaiser, N. Vansteenkiste, and C. Cohen-Tannoudji, Phys. Rev. Lett. **61**, 826 (1988).
[2] M. Kasevich and S. Chu, Phys. Rev. Lett. **67**, 181 (1991).
[3] M. G. Prentiss, N. P. Bigelow, M. S. Shahriar, and P. R. Hemmer, Opt. Lett. **16**, 1695 (1991).
[4] J. Javanainen, Phys. Rev. Lett. **64**, 519 (1990).
[5] H. R. Gray, R. M. Whitley, and C. R. Stroud, Jr., Opt. Lett. **3**, 218 (1978).
[6] P. R. Hemmer, M. G. Prentiss, M. S. Shahriar, and N. P. Bigelow, Opt. Commun. (to be published).
[7] D. Sesko, T. Walker, C. Monroe, A. Gallagher, and C. Wieman, Phys. Rev. Lett. **63**, 961 (1989).
[8] T. Walker, D. Sesko, and C. Wieman, Phys. Rev. Lett. **64**, 408 (1990).
[9] M. S. Shahriar and P. R. Hemmer, Phys. Rev. Lett. **65**, 1865 (1990).
[10] J. Donoghue, M. Cronin-Golomb, J. S. Kane, and P. R. Hemmer, Opt. Lett. **16**, 1313 (1991).
[11] P. R. Hemmer, M. S. Shahriar, V. D. Natoli, and S. Ezekiel, J. Opt. Soc. Am. B **6**, 1519 (1989).
[12] R. Grimm, Y. B. Ovchinnikov, A. I. Sidorov, and V. S. Letokhov, Phys. Rev. Lett. **65**, 1415 (1990).
[13] R. Grimm, Y. B. Ovchinnikov, A. I. Sidorov, and V. S. Letokhov, Opt. Commun. **84**, 18 (1991).
[14] Linear polarization was not used because of problems with optical feedback into the laser.
[15] Similar damping is observed for $\chi=\pi/4$ (not shown).
[16] N. P. Bigelow and M. Prentiss, Phys. Rev. Lett. **65**, 29 (1990).